

On the instantaneous measurement of bloodflow by ultrasonic means

Citation for published version (APA):

Arts, M. G. J. (1971). *On the instantaneous measurement of bloodflow by ultrasonic means*. (EUT report. E, Fac. of Electrical Engineering; Vol. 71-E-20). Technische Hogeschool Eindhoven.

Document status and date:

Published: 01/01/1971

Document Version:

Publisher's PDF, also known as Version of Record (includes final page, issue and volume numbers)

Please check the document version of this publication:

- A submitted manuscript is the version of the article upon submission and before peer-review. There can be important differences between the submitted version and the official published version of record. People interested in the research are advised to contact the author for the final version of the publication, or visit the DOI to the publisher's website.
- The final author version and the galley proof are versions of the publication after peer review.
- The final published version features the final layout of the paper including the volume, issue and page numbers.

[Link to publication](#)

General rights

Copyright and moral rights for the publications made accessible in the public portal are retained by the authors and/or other copyright owners and it is a condition of accessing publications that users recognise and abide by the legal requirements associated with these rights.

- Users may download and print one copy of any publication from the public portal for the purpose of private study or research.
- You may not further distribute the material or use it for any profit-making activity or commercial gain
- You may freely distribute the URL identifying the publication in the public portal.

If the publication is distributed under the terms of Article 25fa of the Dutch Copyright Act, indicated by the "Taverne" license above, please follow below link for the End User Agreement:


www.tue.nl/taverne

Take down policy

If you believe that this document breaches copyright please contact us at:

openaccess@tue.nl

providing details and we will investigate your claim.



th e

ON THE INSTANTANEOUS MEASUREMENT
OF BLOODFLOW BY ULTRASONIC MEANS

by

M.G.J. Arts

ON THE INSTANTANEOUS MEASUREMENT OF BLOODFLOW BY ULTRASONIC MEANS

BY

M.G.J. Arts

TH-Report 71-E-20

ISBN 90 6144 020 3

May 1971

Submitted in partial fulfillment of the requirements
for the degree of Ir. (M.Sc.) at the Eindhoven
University of Technology.

The work was carried out in the Measurement and Control
Group under the directorship of Prof.dr.ir. P. Eykhoff.

Advisor: Ir. J.M.J.G. Roelvros.

ON THE INSTANTANEOUS MEASUREMENT OF BLOODFLOW BY ULTRASONIC MEANS

M.G.J. Arts

Eindhoven University of Technology
Department of Electrical Engineering
Eindhoven, Netherlands

Summary

Part of the problem of determining the flow through a blood vessel is the measurement of the instantaneous average blood velocity over a cross-section of the vessel. In this paper a new method is described to estimate that velocity from the received signal of a doppler flowmeter using continuous ultrasound.

The method is based on the determination of the frequency shift averaged over the power density spectrum of the received signal. Due to a new type of instrumentation this can be done without carrying through a complete frequency analysis of that signal.

This enables a rather accurate determination of the instantaneous value of the blood velocity.

Contents

1. Introduction
 2. The relation between the average velocity across the cross-section of a bloodvessel and the power density spectrum of the received signal.
 3. Differences between mathematical model and reality.
 4. Determination of $\Delta\omega_{av}$ from the receiver signal.
 5. Electronic instrumentation.
 6. The flow instrumentation.
 7. Results.
- Appendix A.
- References.
- Figures.

1. Introduction

For a long time there has been a need for an easy and unbloody way to measure the flow through a bloodvessel. From this point of view, measuring-methods based on the doppler effect of ultrasound, give rise to hopeful expectations.

As a result of the performed study it seems possible, using this effect, to measure the instantaneous velocity of blood, averaged over the cross-section of a bloodvessel. Knowing this average velocity and the diameter of the vessel we compute the flow:

$$\text{Flow} = \text{average velocity} \times \text{cross-section}$$

The determination of the cross-section of a bloodvessel is a separate problem, and will not be discussed in this report.

As mentioned, the principle used for measuring the velocity of blood is based on the doppler effect, appearing when ultrasound, transmitted by a crystal, strikes a moving particle. This particle scatters the sound in all directions. Normally the frequency of the scattered sound differs from the frequency of the transmitted sound. The difference $\Delta\omega$ between the radial frequency of the received and transmitted signal is

$$\Delta\omega = \omega - \omega_0 = \frac{\omega_0}{c} v(\cos\alpha + \cos\beta) \quad (1)$$

with (see fig. 1)

- ω radial frequency of the received signal
- ω_0 radial frequency of the transmitted signal
- c velocity of sound in the medium
- v the velocity of the particle
- α angle between the transmitting beam and the direction of the velocity of the particle
- β angle between the receiving beam and the direction of the velocity of the particle

This principle is already being used for qualitative measurements of the blood flow; the ultrasound will be scattered by the erythrocytes. As a result of the various velocities of these particles (depending on their distance from the axis of the bloodvessel) the received signal contains a spectrum of frequencies. The problem is to determine the average velocity of the blood (averaged over the cross-section of the vessel) from this received signal.

Until now, in doppler flow measuring systems using continuous ultrasound, the received signal is made audible by a loudspeaker by means of synchronous detection. To get a quantitative measurement of the flow, some systems are making use of a zero-crossing technique, applied to the synchronous detected signal (YAO et al. 1970)

It can be shown, however, (Rice 1954) that systems based on this principle fundamentally cannot give accurate measurements of the average velocity of the blood.

In this report a new processing method for the received signal will be described. Because of its theoretical background and the experimental results obtained, this method gives rise to hopeful expectations for unbloody quantitative doppler flow measurements.

2. The relation between the average velocity across the cross-section of a bloodvessel and the power density spectrum of the received signal.

To find the relationship between average velocity and power density spectrum we refer to the situation represented in fig. 2.

The following assumptions are made:

- 1) In the shaded volume inside the bloodvessel, transmitter- and receiverbeam are homogeneous with respect to intensity of radiation and receiving gain respectively.

Moreover these beams are assumed to be sharply bounded.

- 2) Only particles in this volume contribute to the power of the received signal. Every particle is assumed to give the same contribution with respect to the magnitude of this power.

Since in the volume under consideration there are many particles with various velocities, the received signal contains not just one frequency, but a spectrum of frequencies. The particles give equal power contributions, but at different frequencies, depending on the magnitudes of the

quantities in (1).

After trigonometric operation (1) can be written as:

$$\Delta\omega = \omega - \omega_0 = 2 \frac{\omega_0}{c} v \cos\frac{1}{2}(\alpha+\beta)\cos\frac{1}{2}(\alpha-\beta) \quad (2)$$

For a fixed mounting of transmitting and receiving crystals $\cos\frac{1}{2}(\alpha-\beta)$ is a constant. Define a unity vector along the bisector of the angle between transmitter and receiverbeam, pointed between the crystals; c.f. fig. 3. Now one may write:

$$v \cos\frac{1}{2}(\alpha+\beta) = \vec{v} \cdot \vec{k} \quad (3)$$

If a particle has a velocity vector \vec{v}_i one can write for (2):

$$\Delta\omega_i = \omega_i - \omega_0 = 2 \frac{\omega_0}{c} (\vec{k} \cdot \vec{v}_i) \cos\frac{1}{2}(\alpha-\beta) \quad (4)$$

ω_i is the radial frequency component in the received signal, caused by the particle with velocity \vec{v}_i .

Now we define $\Delta\omega_{av}$ as the difference between the average radial frequency of the power density spectrum of the received signal and the radial frequency of the transmitted signal.

Assume that the volume under consideration contains N particles. According to assumption 2) the power contribution to the received signal is equal for every particle, so

$$\Delta\omega_{av} = \frac{1}{N} \sum_{i=1}^N \Delta\omega_i \quad (5)$$

After substitution of (4) in (5) one finds

$$\Delta\omega_{av} = 2 \frac{\omega_0}{c} (\vec{k} \cdot \frac{1}{N} \sum_{i=1}^N \vec{v}_i) \cos\frac{1}{2}(\alpha-\beta) \quad (6)$$

The average velocity of the particles in that volume is

$$\vec{v}_{av} = \frac{1}{N} \sum_{i=1}^N \vec{v}_i \quad (7)$$

Substitution of (7) in (6) results in:

$$\Delta\omega_{av} = 2 \frac{\omega_0}{c} (\vec{k} \cdot \vec{v}_{av}) \cos\frac{1}{2}(\alpha-\beta) \quad (8)$$

Formula (8) relates the average velocity of the particles with the average radial frequencyshift $\Delta\omega_{av}$ of the received signal.

Furthermore we assume:

- The average velocity of the blood in the measuring volume is equal to that across the cross-section of the bloodvessel.
- The concentration of the particles is the same over the whole volume under consideration.
- The velocity of a particle is equal to the velocity of the surrounding liquid.
- The centre of gravity of the cross-section of the bloodvessel remains always in the same place.
- At any moment the bloodvessel is a cylinder (not necessarily a circle-cylinder).

The last one of these assumptions permits us to speak about an axial direction of the blood in the volume under consideration. The fourth assumption implies that the instantaneous average liquid velocity has an axial component only.

All these assumptions together mean that in the volume the instantaneous average liquid velocity is equal to the instantaneous average particle velocity, and that this velocity is axially directed.

Using these assumptions and applying (3) to (8) gives:

$$\Delta\omega_{av} = \frac{\omega_0}{c} (\cos\alpha + \cos\beta)v_{av} \quad (9)$$

- v_{av} The instantaneous average velocity of the blood, averaged over a cross-section of the vessel.
- α The angle between the axis of the vessel and the transmitter beam.
- β The angle between the axis of the vessel and the receiver beam.

According to the definition for the average radial frequency shift one may write:

$$\Delta\omega_{av} = \frac{\int_0^{\infty} \omega\phi(\omega) d\omega}{\int_0^{\infty} \phi(\omega) d\omega} - \omega_0 \quad (10)$$

where $\phi(\omega)$ is the spectral power density of the received signal as a function of the radial frequency ω .

If v_m is the maximum velocity of a blood particle ever expected in a bloodvessel, one may write:

$$|\Delta\omega| = |\omega - \omega_0| < \Delta\omega_m = 2 \frac{\omega_0}{c} v_m$$

This means $\phi(\omega) \equiv 0$ for $||\omega| - \omega_0| > \Delta\omega_m$ (11)

After substitution of $\omega = \omega_0 + \Delta\omega$ equation (10) changes into:

$$\Delta\omega_{av} = \frac{\int_{-\Delta\omega_m}^{+\Delta\omega_m} \Delta\omega \cdot \phi(\omega_0 + \Delta\omega) d\Delta\omega}{\int_{-\Delta\omega_m}^{+\Delta\omega_m} \phi(\omega_0 + \Delta\omega) \cdot d\Delta\omega} \quad (12)$$

Equation (12) shows a way to determine $\Delta\omega_{av}$ from the power density spectrum of the received signal. If $\Delta\omega_{av}$ is known and also the angles α and β , one can determine the average velocity of the blood in the cross-section by means of expression (9).

3. Differences between mathematical model and reality

A number of assumptions, more or less agreeing with reality, were made in the derivation of eq. (9) for the average velocity of the blood. The implications of these assumptions will be discussed now.

- In general the transmitting- and receiving crystals will have radiation patterns which are not homogeneous in the main beam. Moreover the vessel wall and the surrounding tissue have acoustic properties that differ from the acoustic properties of blood.

This causes diffraction and reflection of ultrasound. For this reason the sound intensity in the volume of the bloodvessel is not homogeneous.

The averaging of the velocities of the particles over the cross-section by means of the spectral power density of the received signal, gives rise to errors, as velocities in places with a higher sound intensity give relatively too much power contribution.

It is expected, however, that when using crystals with good beam properties, these errors will not be large, since also the acoustical properties of tissue, vessel wall and blood do not differ very much.

- In addition to the moving erythrocytes all kind of tissue discontinuities (for instance the moving vessel wall) will give a contribution to the power of the received signal.

The contribution of the discontinuities at rest, which is found in the spectral power density at the radial frequency ω_0 , will be very large and has to be eliminated.

The slowly moving vessel wall will also give a contribution at shifted frequencies. As the velocities of the vessel wall are small, the contributions of the vessel wall will be close to ω_0 . (dependent on the angles α and β)

Elimination of these frequencies, which also eliminates the power contribution of slowly moving erythrocytes) is necessary. A correction for the error caused by this elimination will be discussed later.

- In fact the average particle velocity is measured. Because of the non-homogeneous particle concentration and a relative movement of the particles with respect to the carrier flow, this velocity need not be equal to the average blood velocity.

In an experimental set-up a number of power density spectra were measured in order to estimate the errors which occur due to the assumptions made for the mathematical model. This has been done in situations with stationary flow and different values for the angles α and β . From these spectra the average frequency difference $\Delta\omega_{av}$ was determined and using formula (9) the average velocity was calculated.

At normal velocities (20 cm/sec) and favourable angles α and β ($30^\circ < \alpha, \beta < 60^\circ$) the difference between the calculated and the real velocity was less than 5%.

Stimulated by this interesting result, we directed research toward finding a fast and accurate method to determine $\Delta\omega_{av}$ from the received signal.

Fig. 4 gives some measured power density spectra. They are recorded for the case of a stationary and laminary flow of a latex in water suspension through a thin-walled latex tube, at different angles $\frac{1}{2}(\alpha+\beta)$.

4. Determination of $\Delta\omega_{av}$ from the receiver signal.

Starting point for this determination is the expression (12) for $\Delta\omega_{av}$. The numerator and denominator of this expression are determined separately and after that the division is performed.

The most obvious method to determine the numerator and denominator is to perform the integrations in expression (12) over the power density function of the receiversignal. In that case a frequency analyser has to be used to produce this spectrum. This method was used in the first experiments.

It is possible, however, to realize numerator and denominator as D.C. components of time signals which can be derived from the receiver signal directly. The mathematical exposition of this method will be given first. In this explanation some properties of fourier transformation will be used. These properties are given in appendix A.

Determination of the denominator (see fig. 5)

Assume the receiver signal $f(t)$ has a fourier transform $F(\omega)$. As stated before the receiver signal contains only frequencies in a band around ω_0

$$F(\omega) \equiv 0 \quad \text{for} \quad ||\omega - \omega_0| > \Delta\omega_m \quad (13)$$

In a synchronous detector the receiver signal $f(t)$ is multiplied by $\cos\omega_0 t$.

$$f_{D1}(t) = f(t) \cos\omega_0 t = \frac{1}{2} f(t) \{e^{i\omega_0 t} + e^{-i\omega_0 t}\}$$

According to formula (e) of appendix A the fourier transform of $f_{D1}(t)$ is

$$F_{D1}(\omega) = \frac{1}{2}\{F(\omega - \omega_0) + F(\omega + \omega_0)\}$$

$$F_{D1}(\omega) \equiv 0 \quad \text{for} \quad \begin{array}{l} |\omega| > 2\omega_0 + \Delta\omega_m \\ \Delta\omega_m < |\omega| < 2\omega_0 - \Delta\omega_m \end{array} \quad (14)$$

The output signal of the detector passes through a low pass filter which eliminates the frequencies in the bands around $|\omega| = 2\omega_0$.

The output of this filter is $f_{L1}(t)$ and its fourier transform is

$$F_{L1}(\omega) = \frac{1}{2}\{F(\omega-\omega_0) + F(\omega+\omega_0)\} \quad (15)$$

$$F_{L1}(\omega) \equiv 0 \quad \text{for} \quad |\omega| > \Delta\omega_m$$

The square of $f_{L1}(t)$ is

$$d(t) = f_{L1}^2(t) \quad (16)$$

and according to formula (d) of the appendix, its fourier transform is

$$D(\omega) = \frac{1}{2\pi} \int_{-\infty}^{+\infty} F_{L1}(w) F_{L1}(\omega-w) dw$$

The DC component of $d(t)$ is $D(0)$; using formule (c) of the appendix, one finds:

$$D(0) = \frac{1}{2\pi} \int_{-\infty}^{+\infty} F_{L1}(w) F_{L1}^*(+w) dw \quad (17)$$

and after substitution of (15)

$$D(0) = \frac{1}{8\pi} \int_{-\Delta\omega_m}^{+\Delta\omega_m} \{F(w-\omega_0)F^*(w-\omega_0) + F(w+\omega_0)F^*(w+\omega_0)\} dw \quad (18)$$

$$+ \frac{1}{8\pi} \int_{-\Delta\omega_m}^{+\Delta\omega_m} \{F(w-\omega_0)F^*(w+\omega_0) + F(w+\omega_0)F^*(w-\omega_0)\} dw$$

Only if there are particles in the volume with opposite velocities, the product terms in the second integral of (18) are not equal zero.

In that case, however, the expected contribution of this integral to $D(0)$ will still be zero, as the frequency components $F(\omega-\omega_0)$ and $F^*(\omega+\omega_0)$, caused by these particles, are not correlated in time.

So using formula (f) of the appendix and remembering that the spectral density $\phi(\omega) = F(\omega)F^*(\omega)$ of the receiver signal is an even function of ω , one finds:

$$D(0) = \frac{1}{8\pi} \int_{-\Delta\omega_m}^{+\Delta\omega_m} \phi(w+\omega_0) + \phi(w-\omega_0) dw = \frac{1}{4\pi} \int_{-\Delta\omega_m}^{+\Delta\omega_m} \phi(\omega_0+w) dw \quad (19)$$

Consequently $4\pi D(0)$ equals the denominator of formule (12) and can be used for the determination of $\Delta\omega_{av}$.

Determination of the numerator.

For the determination of the numerator of (12) the receiver signal $f(t)$ is multiplied by $\sin\omega_0 t$ in a synchronous detector, of which the output is

$$f_{D2}(t) = f(t)\sin\omega_0 t = \frac{1}{2i} f(t) \{ e^{i\omega_0 t} - e^{-i\omega_0 t} \}$$

The fourier transform of $f_{D2}(t)$ is

$$F_{D2}(\omega) = \frac{1}{2i} \{ F(\omega - \omega_0) - F(\omega + \omega_0) \} \quad (20)$$

$f_{D2}(t)$ passes a low pass filter to eliminate frequencies around $|\omega| = 2\omega_0$. The output signal of this filter is $f_{L2}(t)$, which has a fourier transform

$$F_{L2}(\omega) = \frac{1}{2i} \{ F(\omega - \omega_0) - F(\omega + \omega_0) \} \quad (21)$$

$$F_{L2}(\omega) \equiv 0 \text{ for } |\omega| > \Delta\omega_m$$

Now

$$f_{L3}(t) = \frac{d}{dt} f_{L2}(t) \quad (22)$$

According to formula (g) of the appendix, the fourier transform of $f_{L3}(t)$ is

$$F_{L3}(\omega) = i\omega F_{L2}(\omega) = \frac{1}{2} \omega \{ F(\omega - \omega_0) - F(\omega + \omega_0) \} \quad (23)$$

$$F_{L3}(\omega) \equiv 0 \text{ for } |\omega| > \Delta\omega_m$$

Forming the product of $f_{L1}(t)$ and $f_{L3}(t)$, one finds

$$n(t) = f_{L1}(t) \cdot f_{L3}(t) \quad (24)$$

Using formula (d) of the appendix, the fourier transform of $n(t)$ is found to be:

$$N(\omega) = \frac{1}{2\pi} \int_{-\infty}^{+\infty} F_{L1}(w) F_{L3}(\omega - w) dw$$

The D.C. component of $n(t)$ is $N(0)$; using formula (c) of the appendix, one finds

$$N(0) = \frac{1}{2\pi} \int_{-\infty}^{+\infty} F_{L1}(w) F_{L3}^*(w) dw \quad (25)$$

Substitution of (24) and (15) gives:

$$N(0) = \frac{1}{8\pi} \int_{-\Delta\omega_m}^{+\Delta\omega_m} w \{ F(w-\omega_0) F^*(w-\omega_0) - F(w+\omega_0) F^*(w+\omega_0) \} dw$$

$$+ \frac{1}{8\pi} \int_{-\Delta\omega_m}^{+\Delta\omega_m} w \{ F(w+\omega_0) F^*(w-\omega_0) - F(w-\omega_0) F^*(w+\omega_0) \} dw \quad (26)$$

For the same reason as given in the explanation for (18) the second integral in (26) gives no average contribution to $N(0)$, and one can write for $N(0)$

$$N(0) = \frac{1}{8\pi} \int_{-\Delta\omega_m}^{+\Delta\omega_m} w \{ \Phi(w-\omega_0) - \Phi(w+\omega_0) \} dw$$

$$= -\frac{1}{4\pi} \int_{-\Delta\omega_m}^{\Delta\omega_m} w \Phi(w+\omega_0) dw \quad (27)$$

Consequently $-4\pi N(0)$ equals the numerator of expression (12) and can be used for the determination of $\Delta\omega_{av}$.

5. Electronic Instrumentation

The method described makes it possible to determine the average velocity over a cross-section of a tube as a function of time. The instrumentation that follows from the mathematical description is given in fig. 5.

For good functioning in practice, however, this instrumentation needs some additions, which will be described now.

1. High Frequency Amplifier.

As the received signal $f(t)$ is too small, it has to be amplified, in order to get a sufficient amplitude for the demodulation multipliers.

2. Automatic Volume Control.

The magnitude of the received signal can vary considerably under

different circumstances. This means that also the magnitude of $f_{L1}(t)$ and $f_{L2}(t)$ vary.

Because of the limited driving range of the multipliers and the divider, an automatic volume control for the denominator is used. As the ratio of the signals $f_{L1}(t)$ and $f_{L2}(t)$ may not be influenced, two coupled volume controls are used. These are part of an integrating control system which keeps the D.C. component of $d(t)$ at a constant value (see fig. 7).

The constant value of this component seems to make the divider redundant. However experiments showed that the output of the divider had less noise than the numerator, and therefore it was still used.

3. Limitation of the pass band for the low frequency signals.

As mentioned before, the power spectral density $\Phi(\omega)$ of the receiver signal is very large for frequencies close to ω_0 . This is caused by reflections of the ultrasound by stationary or by slowly moving tissue transitions (e.g. bloodvessel wall and skin).

When determining the average velocity from $\Phi(\omega)$ this would cause large errors. That is why the frequencies close to ω_0 have to be eliminated. To realize that, the low pass filters after the synchronous detectors (see fig. 5) have to be replaced by band pass filters.

The high cut-off frequency of these filters is still $\Delta\omega_m$. The low cut-off frequency $\Delta\omega_L$ is that frequency above which there is no important power contribution from reflecting subjects except from blood particles.

This way of filtering implies the elimination of the lowest frequencies, that are caused by the moving blood particles, and so a change of $\Delta\omega_{av}$ into $\Delta\omega'_{av}$. In fig. 6 the apparent consequences of this filtering for $\Phi(\omega)$ are given, and corrections are made to keep the difference between $\Delta\omega_{av}$ and $\Delta\omega'_{av}$ small.

By artificially raising the power contribution of the frequencies with a shift between $\Delta\omega_L$ and $\Delta\omega_c$, the difference between $\Delta\omega_{av}$ and $\Delta\omega'_{av}$ is smaller for receiver signals that have a maximum frequency larger than $\omega_0 + \Delta\omega_c$. For signals with a maximum frequency lower than this value, however, the error is still the same.

By creating negative frequency shifts in the region $-\Delta\omega_L \rightarrow -\Delta\omega_C$ the error made for the last signals is kept small too.

For signals with a maximum frequency lower than $\omega_0 + \Delta\omega_L$ there is no correction at all. This frequency determines the lowest velocity that can be measured.

The raising of the lowest frequencies is easy to realize in the band pass filters which have to be identical for both channels. The negative frequency shifts are artificially created by admitting cross-talk for the lowest frequencies of $f_{L1}(t)$ and $f_{L2}(t)$ (see fig. 7).

4. Zero-calibration.

During measurements a zero-calibration can be done at any moment when a flow is present. This calibration is made by connecting the signal lines of $f_{L1}(t)$ and $f_{L2}(t)$.

As the D.C. component of $g(t) \cdot \frac{d}{dt} g(t)$ is zero, the output of the divider has to be zero in the case of connection. This gives a way to set the offset of the divider to zero.

The block-diagram of the system after all these modifications is given in fig. 7.

Calculation of the average frequency shift by using the signals $N(t)$ and $D(t)$.

It has been shown that the numerator and denominator of eq. (4) are equal to the DC-components of the signals $-2 n(t)$ respectively $2 d(t)$. To determine the D.C.-component of a signal it is necessary to average over an infinite time interval. Since changes in the velocity also should be measured, the D.C.-component only can be estimated by averaging over a finite time interval. This interval is determined by the maximum frequency of the changes of the velocity that have to be measured. Of course, by averaging over a shorter interval the estimation is less accurate and the noise will be larger.

Analogously in time this averaging across a short period can be done by a low pass filter without oscillations in the impulse response. The radial cut-off frequency should be equal to about the reciprocal of the wanted averaging period.

6. The flow instrumentation.

To verify the measuring system it is necessary to design a flow instrumentation, which resembles as much as possible reality.

The blood vessel is simulated by a small latex-rubber tube, stretched till double the length. In this case the measurements of the tube are: diameter inside about 4 mm, thickness of the wall about 0,15 mm and length about 150 mm.

A good simulation for the blood is a suspension in water of small latex spheres, of the size of the erythrocytes. Before using, this suspension is boiled under very low pressure to remove small bubbles of gas.

Comparing the measuring results obtained with blood and this liquid, it appeared that the scattering properties of both liquids were the same.

To simulate the surrounding tissue the tube is placed in a basin filled with water. In this basin also is placed the holder, keeping the transmitter and receiver crystal. By turning this holder around the centre of the artificial blood vessel, the angle $\frac{1}{2}(\alpha+\beta)$ can be changed (see fig. 8)

All the quantitative measurements have been performed on stationary laminary flow. For these measurements it is necessary to keep the velocity of the liquid constant during some time. This velocity is determined by a constant difference between two levels (see fig. 9).

The lower level is constant because of overflow of the reservoir B, into which the liquid is flowing. The upper level is constant, since the loss of weight of the reservoir A as a result of the loss of liquid, causes a contraction of the spring, just enough to keep the level constant.

During the doppler velocity measurement, the innerdiameter d of the latex tube was measured too.

Also measured was the time interval T_v required for a known volume V to flow from resevoir A.

The average velocity over the cross-section of the latex tube can be computed.

$$v_{av} = \frac{V}{T_v} \cdot \frac{4}{\pi d^2} \quad (28)$$

This should be equal to the average velocity measured with the doppler method.

7. Results

The output voltage of the described velocity meter is proportional to the average frequency shift of the received signal, compared with the transmitter frequency.

According to eq. (9) this average frequency shift is proportional to $v_{av}(\cos\alpha + \cos\beta)$. Knowing ω_o and c one can calculate $v_{av}(\cos\alpha + \cos\beta)$ from the output signal.

The angles α and β can be measured and therefore $v_{av}(\cos\alpha + \cos\beta)$ can be calculated too from eq. (28).

These two values are compared for 72 cases in fig. 10.

The heavy lines represent the relationship between the computed value of $v_{av}(\cos\alpha + \cos\beta)$ and $\frac{1}{2}(\alpha+\beta)$ for eight values of the flow.

For each flow the output voltage of the velocity meter was measured for nine values of the angle $\frac{1}{2}(\alpha+\beta)$. After calibration these measuring points were indicated in the same figure.

Quantitative verification of measurements in the case of dynamic flow, however, has not yet been done.

Appendix A

If $f(t)$ is a function of a real variable t , and the integral $\int_{-\infty}^{+\infty} |f(t)| dt$ exists, the fourier transform of $f(t)$ exists and is noted as

$$f(t) \text{ o-o } F(\omega)$$

The fourier transform $F(\omega)$ is defined as

$$F(\omega) = \int_{-\infty}^{+\infty} f(t) e^{-i\omega t} dt \tag{a}$$

From $F(\omega)$, $f(t)$ can be found as

$$f(t) = \frac{1}{2\pi} \int_{-\infty}^{+\infty} F(\omega) e^{i\omega t} d\omega \tag{b}$$

In general $F(\omega)$ is complex

$$F(\omega) = R(\omega) + ix(\omega)$$
$$F^*(\omega) = R(\omega) - ix(\omega)$$

Properties

If $f(t)$ is a real function of t , then

$$F^*(\omega) = F(-\omega) \tag{c}$$

If $f(t) \text{ o-o } F(\omega)$ and $g(t) \text{ o-o } G(\omega)$, then

$$f(t) \cdot g(t) \text{ o-o } \frac{1}{2\pi} \int_{-\infty}^{+\infty} F(\omega) G(\omega - \omega') d\omega \tag{d}$$

If $f(t) \text{ o-o } F(\omega)$ then

$$f(t) \cdot e^{i\omega_0 t} \text{ o-o } F(\omega - \omega_0) \tag{e}$$

If $f(t) \text{ o-o } F(\omega)$ then

$$\frac{d}{dt} f(t) \text{ o-o } i\omega F(\omega) \tag{g}$$

The spectral powerdensity of a signal $f(t)$ which has a fourier transform $F(\omega)$ is

$$\Phi(\omega) = F(\omega) \cdot F^*(\omega) \tag{f}$$

LINDHOVEN UNIVERSITY OF TECHNOLOGY
THE NETHERLANDS
DEPARTMENT OF ELECTRICAL ENGINEERING

TH-Reports:

1. Dijk, J., M. Jeuken & E.J. Maanders
AN ANTENNA FOR A SATELLITE COMMUNICATION GROUND STATION
(PROVISIONAL ELECTRICAL DESIGN). TH-report 68-E-01. March 1968.
2. Veefkind, A., J.H. Blom & L.H.Th. Rietjens
THEORETICAL AND EXPERIMENTAL INVESTIGATION OF A NON-EQUILIBRIUM PLASMA
IN A MHD CHANNEL. TH-report 68-E-02. March 1968. Submitted to the
Symposium on Magnetohydrodynamic Electrical Power Generation, Warsaw,
Poland, 24-30 July, 1968.
3. Boom, A.J.W. van den & J.H.A.M. Melis
A COMPARISON OF SOME PROCESS PARAMETER ESTIMATING SCHEMES.
TH-report 68-E-03. September 1968.
4. Eykhoff, P., P.J.M. Ophay, J. Severs & J.O.M. Oome
AN ELECTROLYTIC TANK FOR INSTRUCTIONAL PURPOSES REPRESENTING THE
COMPLEX-FREQUENCY PLANE. TH-report 68-E-04. September 1968.
5. Vermij, L. & J.E. Daalder
ENERGY BALANCE OF FUSING SILVER WIRES SURROUNDED BY AIR,
TH-report 68-E-05. November 1968.
6. Houben, J.W.M.A. & P. Massee
MHD POWER CONVERSION EMPLOYING LIQUID METALS.
TH-report 69-E-06. February 1969.
7. Heuvel W.M.C. van den & W.F.J. Kersten
VOLTAGE MEASUREMENT IN CURRENT ZERO INVESTIGATIONS.
TH-report 69-E-07. September 1969.
8. Vermij, L.
SELECTED BIBLIOGRAPHY OF FUSES. TH-report 69-E-08. September 1969.

9. Westenberg, J.Z.
SOME IDENTIFICATION SCHEMES FOR NON-LINEAR NOISY PROCESSES.
TH-report 69-E-09. December 1969.
10. Koop, H.E.M., J. Dijk & E.J. Maanders
ON CONICAL HORN ANTENNAS. TH-report 70-E-10. February 1970.
11. Veefkind, A.
NON-EQUILIBRIUM PHENOMENA IN A DISC-SHAPED MAGNETOHYDRODYNAMIC GENERATOR
TH-report 70-E-11. March 1970.
12. Jansen, J.K.M., M.E.J. Jeuken & C.W. Lambrechtse
THE SCALAR FEED. TH-report 70-E-12. December 1969.
13. Teuling, D.J.A.
ELECTRONIC IMAGE MOTION COMPENSATION IN A PORTABLE TELEVISION CAMERA.
TH-report 70-E-13. 1970.
14. Lorencin, M.
AUTOMATIC METEOR REFLECTIONS RECORDING EQUIPMENT.
TH-report 70-E-14. November 1970.
15. Smets, A.J.
THE INSTRUMENTAL VARIABLE METHOD AND RELATED IDENTIFICATION SCHEMES.
TH-report 70-E-15. November 1970.
16. White Jr., R.C.
A SURVEY OF RANDOM METHODS FOR PARAMETER OPTIMIZATION.
TH-report 70-E-16. February 1971.
17. Talmon, J.L.
APPROXIMATED GAUSS-MARKOV ESTIMATORS AND RELATED SCHEMES.
TH-report 71-E-17. February 1971.
18. Kalásek, V.K.
MEASUREMENTS OF TIME CONSTANTS ON CASCADE D.C. ARE IN NITROGEN.
TH-report 71-E-18. February 1971.
19. Hosselet, L.M.L.F.
OZONBILDUNG MITTELS ELEKTRISCHE ENTLADUNGEN.
TH-report 71-E-19. April 1971.

References

YAO, S.T. et al (1970) Transcutaneous measurement of bloodflow by ultrasound. Bio-Med. Eng. 5, 230-233.

RICE, S.O. (1954). In: Selected papers on noise and stochastic processes. Ed. N. WAX. pag. 189, Dover Publications, New York.

- Fig. 1 Doppler effect of ultrasound on a moving particle.
- Fig. 2 Volume part of the vessel under consideration.
- Fig. 3 Scattering of ultrasound on a bloodparticle in a vessel.
- Fig. 4 Examples of power density spectra measured in the model.
- Fig. 5 Block diagram of the measuring system.
- Fig. 6 Consequences of band pass filtering and corrections.
- Fig. 7 Block diagram of the measuring system with completions.
- Fig. 8 Schematic view of the arteficial artery and the crystals.
- Fig. 9 The flow system
- Fig. 10 Measuring results at different angles $\frac{1}{2}(\alpha+\beta)$

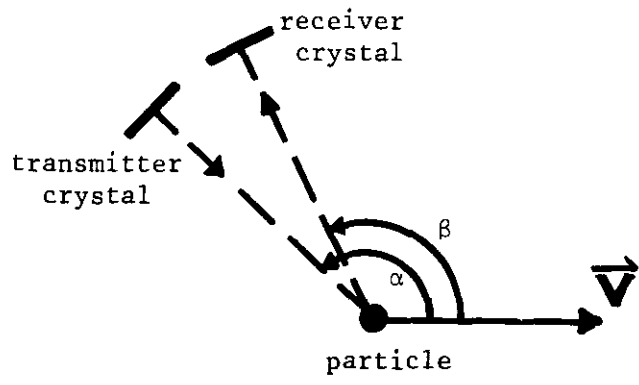


Fig. 1

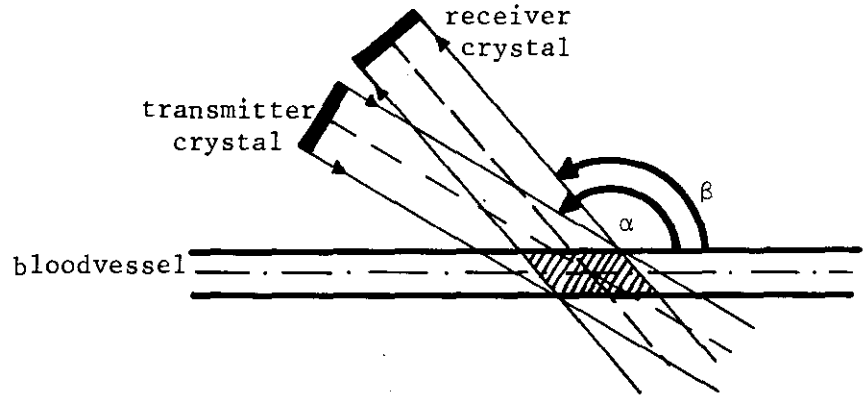


Fig. 2

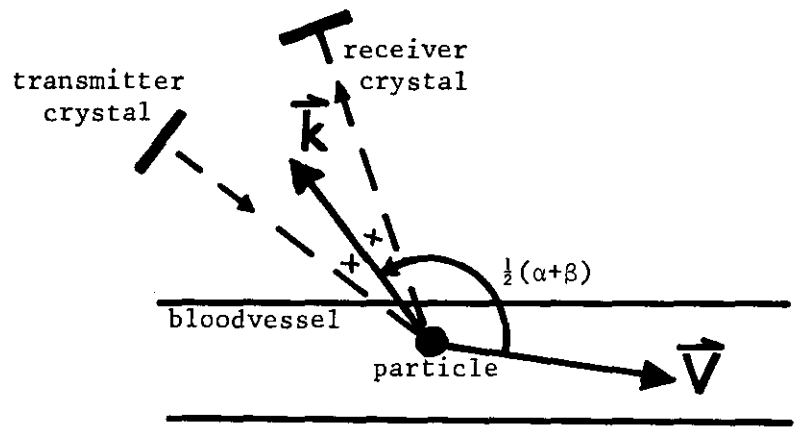
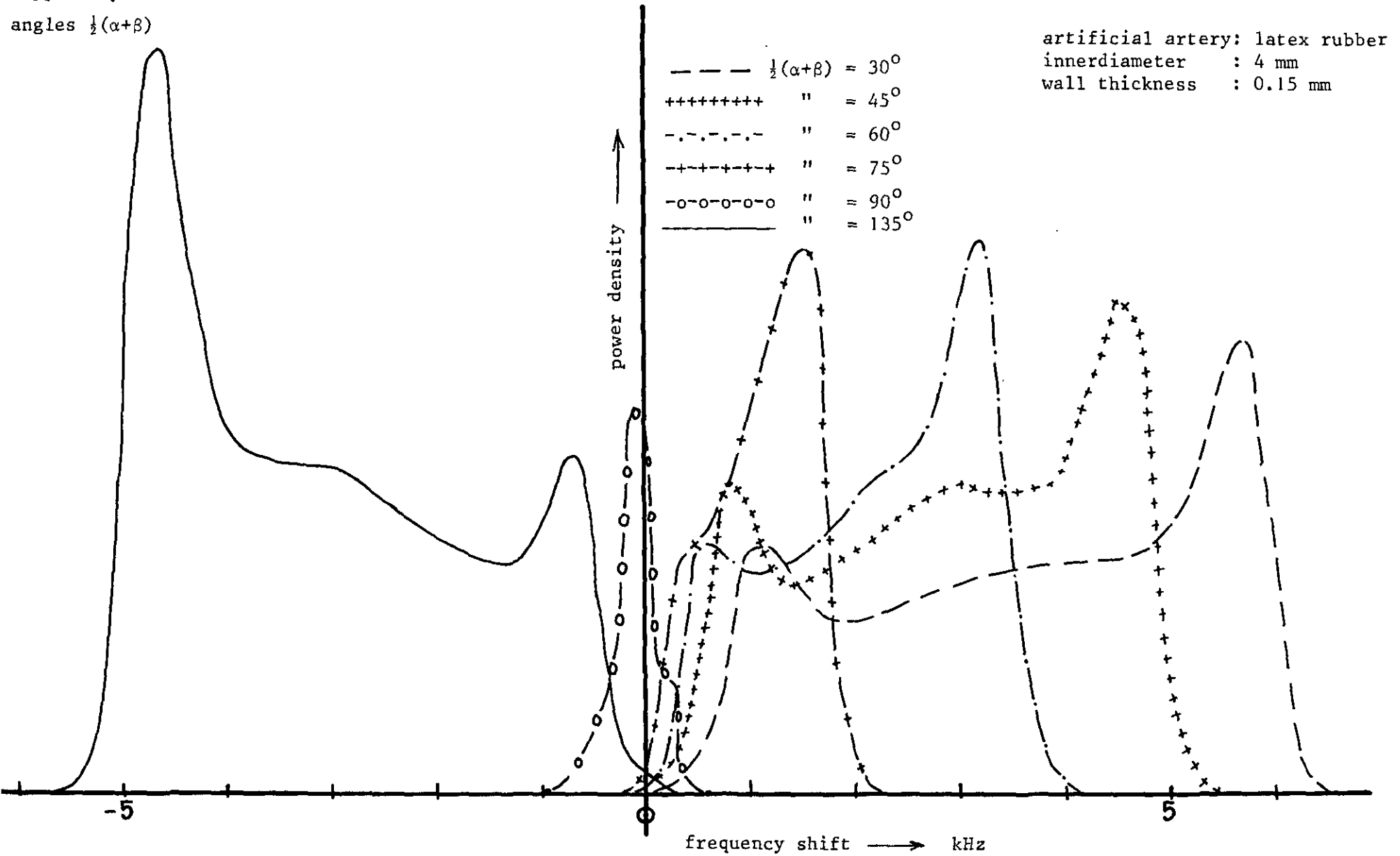


Fig. 3

Fig. 4

Doppler spectra at constant flow but different angles $\frac{1}{2}(\alpha+\beta)$



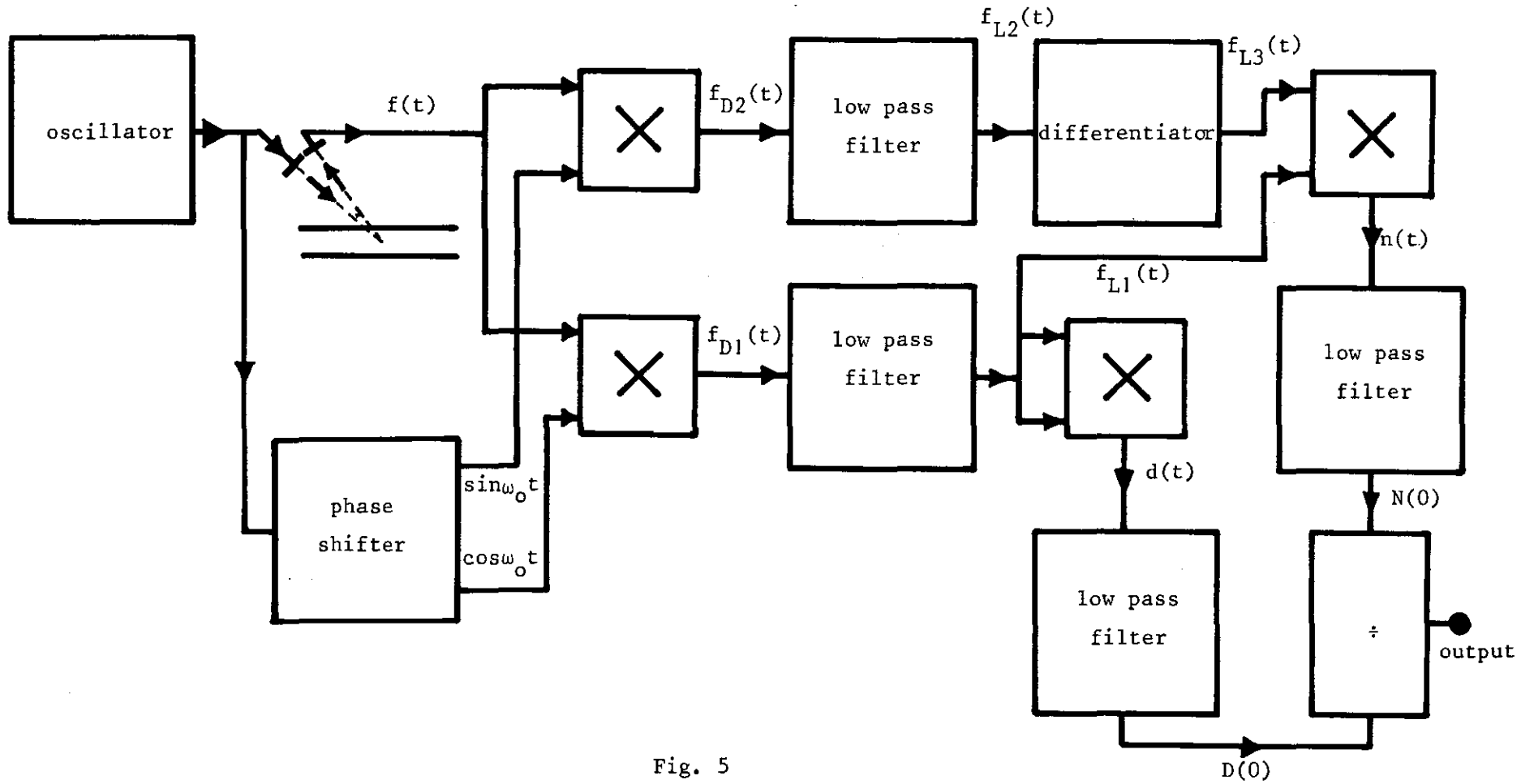
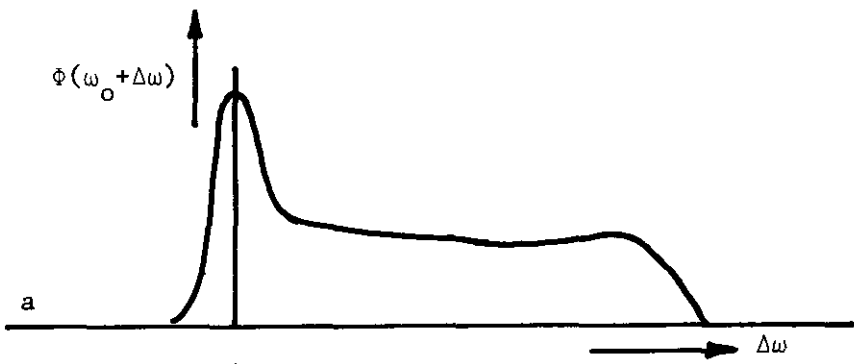
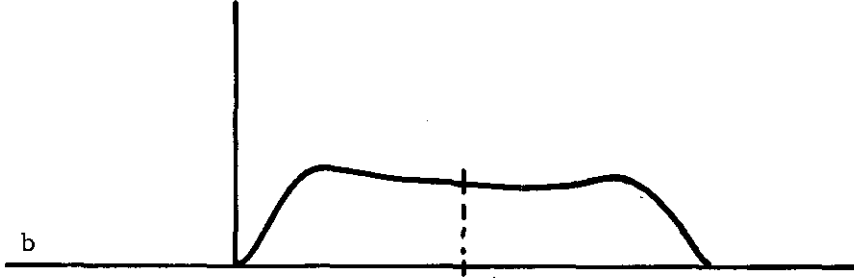


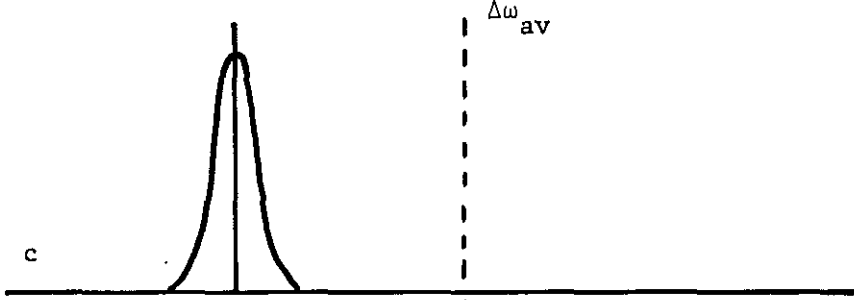
Fig. 5



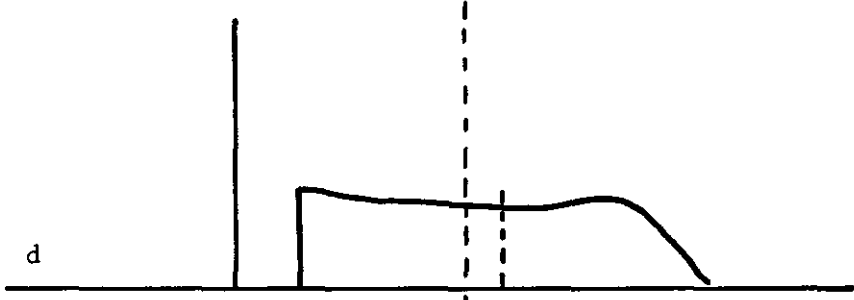
Power density spectrum
 $\Phi(\omega_0 + \Delta\omega)$ of the receiver
 signal around $\omega = \omega_0$.



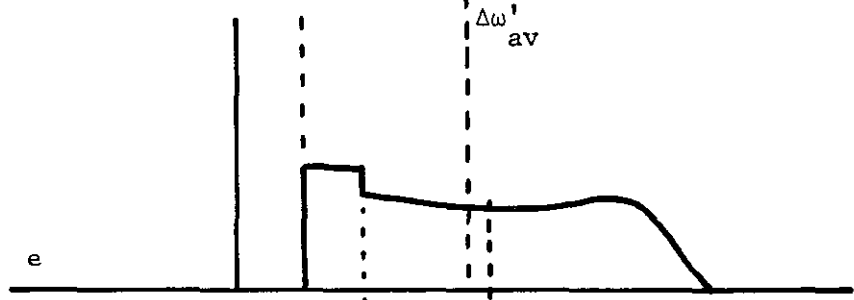
Contribution of the moving
 particles to $\Phi(\omega_0 + \Delta\omega)$



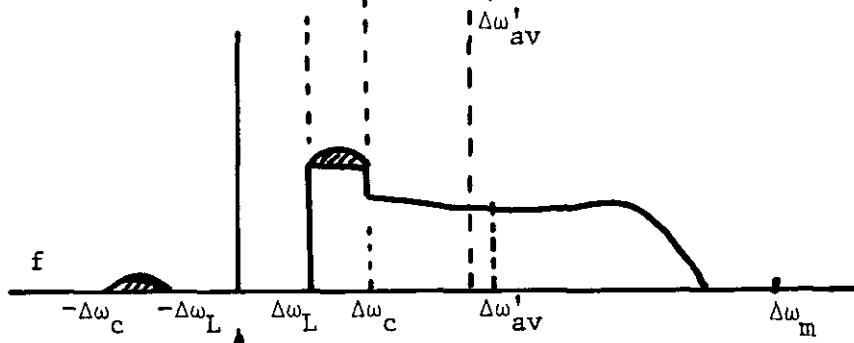
Contribution of stationary
 and slowly moving transi-
 tions



Contribution of the moving
 particles after bandpass
 filtering.



Correction for signals with
 a maximum frequency
 $> \omega_0 + \Delta\omega_c$



Correction for signals with
 a maximum frequency
 $\omega_0 + \Delta\omega_L < \omega < \omega_0 + \Delta\omega_c$

$\Delta\omega = 0$
 $\omega = \omega_0$

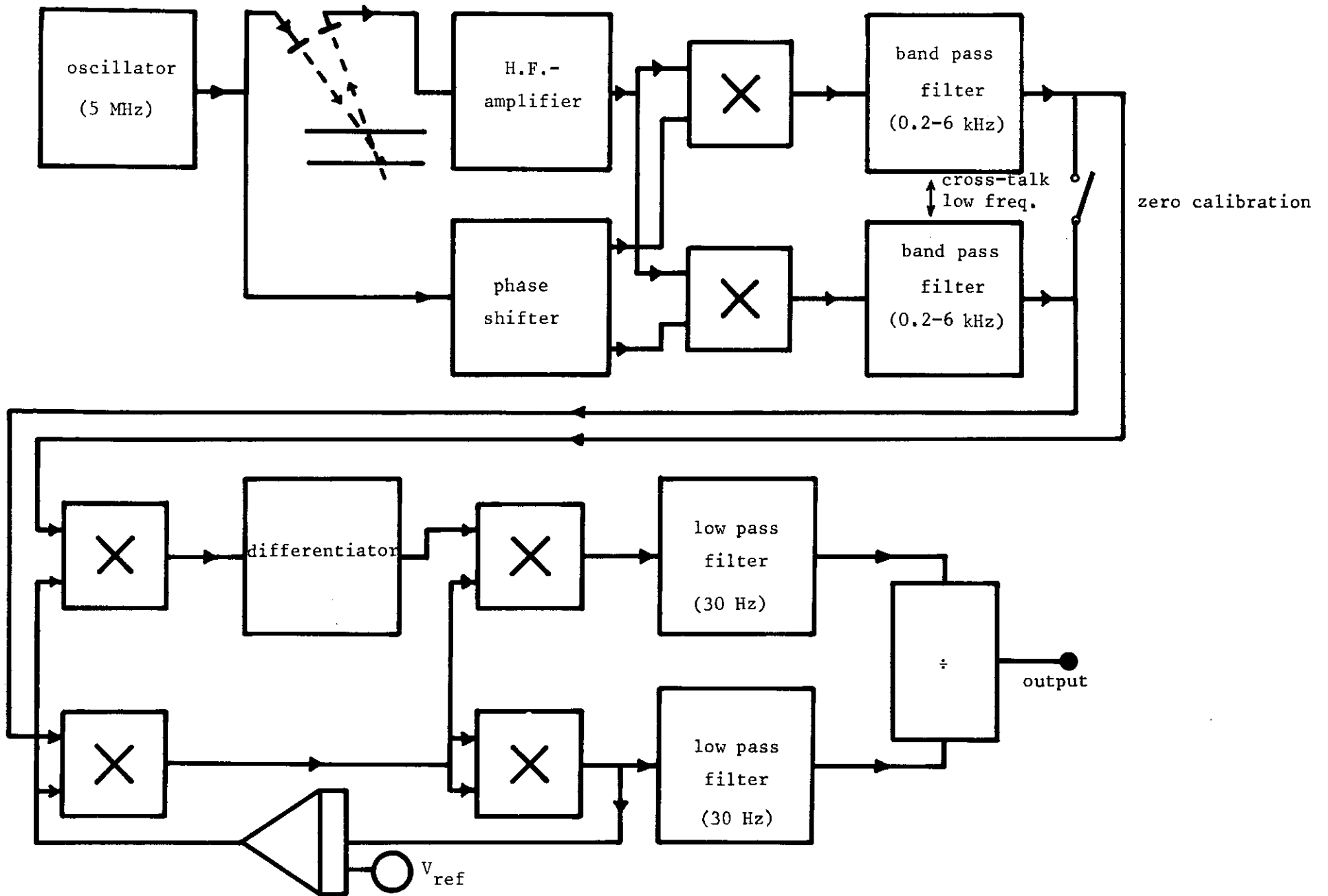


Fig. 7

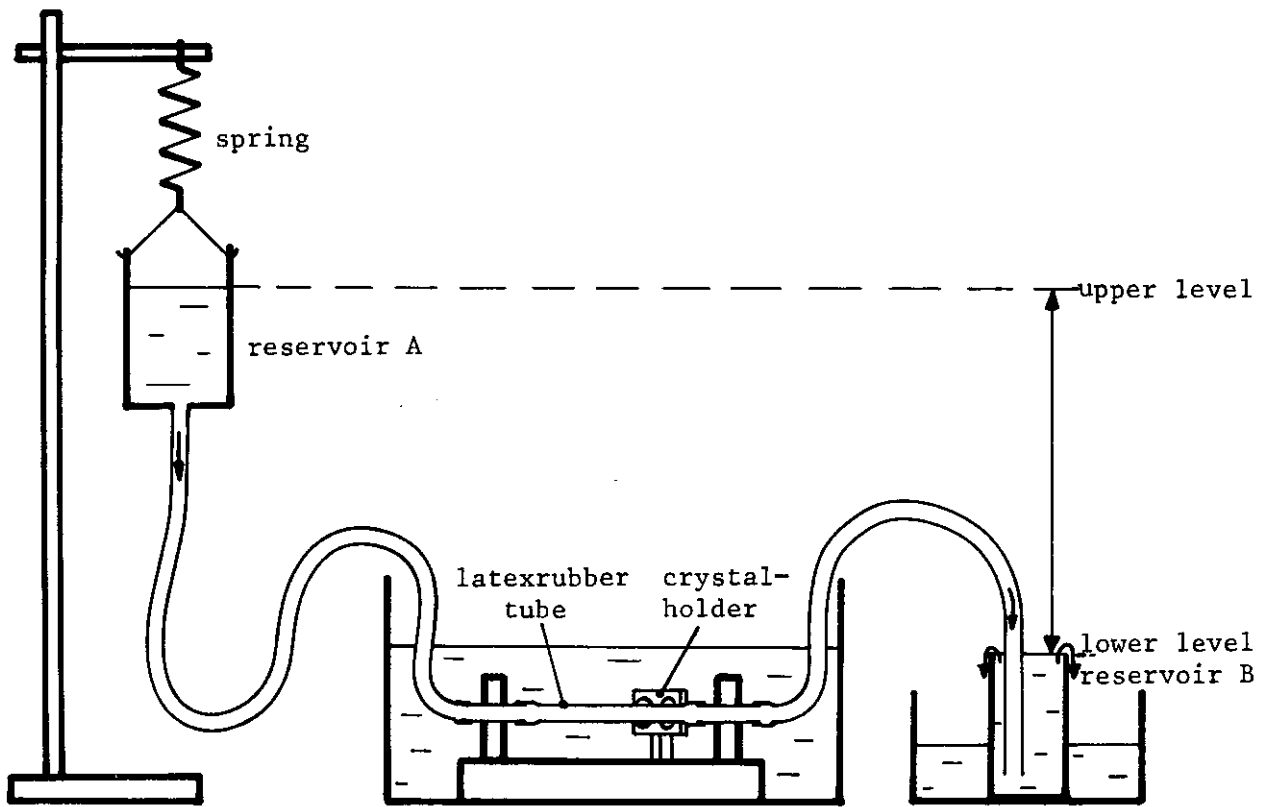


Fig. 9

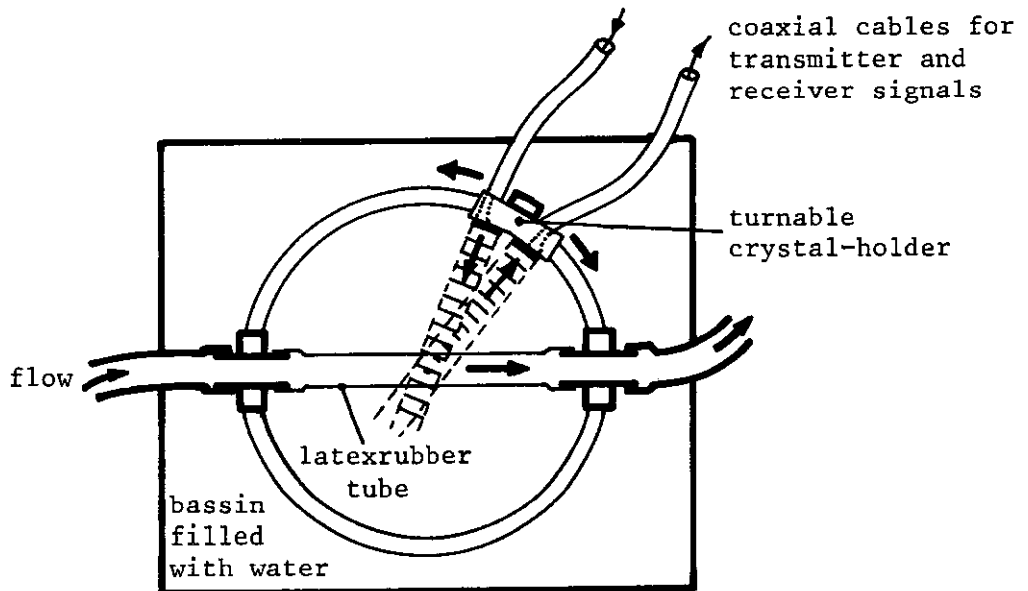


Fig. 8

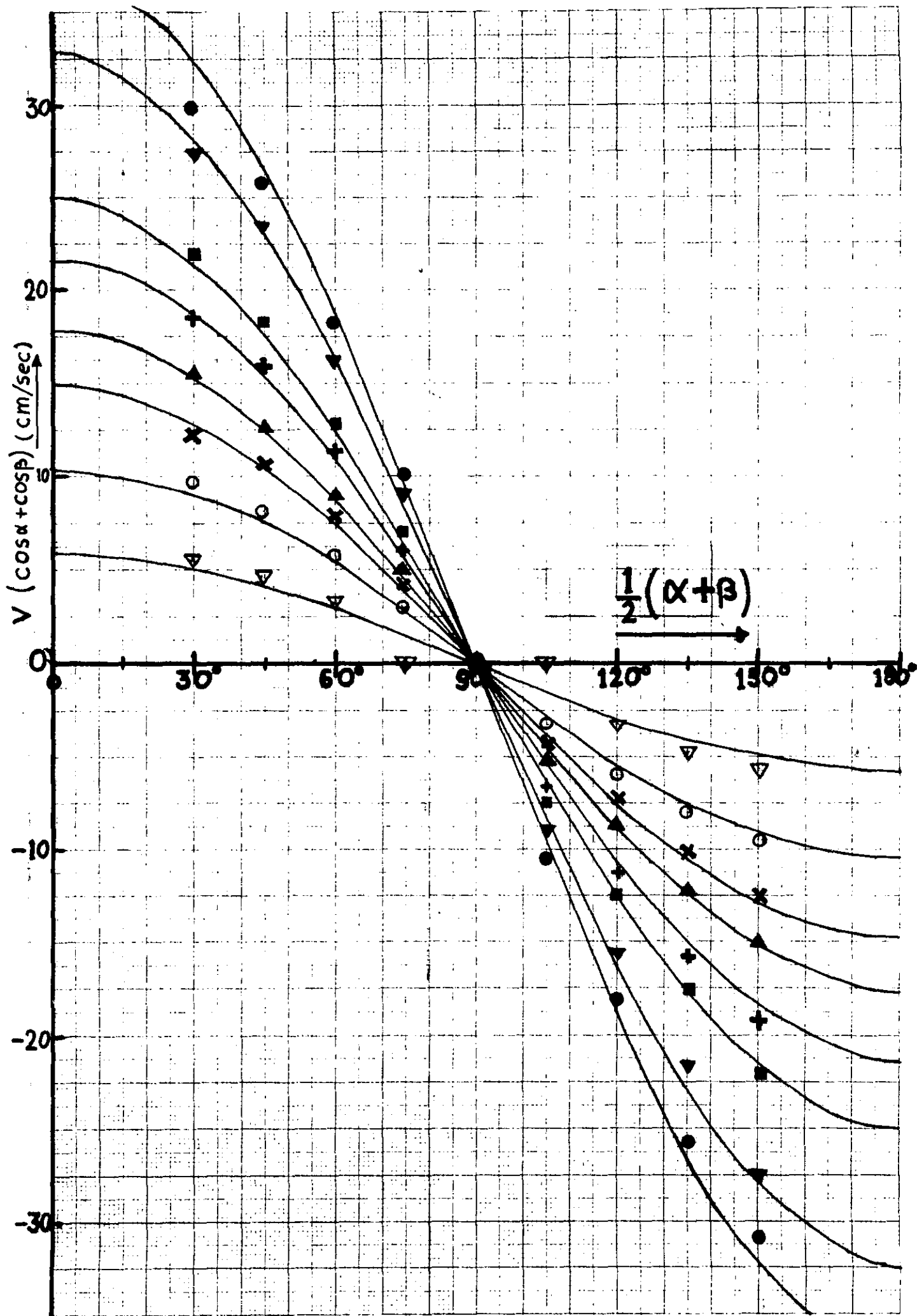


fig. 10